RESEARCH FRONT

CSIRO PUBLISHING

Aust. J. Chem.
http://dx.doi.org/10.1071/CH14326

Full Paper

Assembly of Layer-Type Organosilver(I) Complexes Incorporating Nitrate and Isomeric Halophenylethynide Ligands

Ping-Shing Cheng,[A] *Sam C. K. Hau,*[A] *and Thomas C. W. Mak*[A,B]

[A]Department of Chemistry and Center of Novel Functional Molecules, The Chinese University of Hong Kong, Shatin, New Territories, Hong Kong SAR, China.
[B]Corresponding author. Email: tcwmak@cuhk.edu.hk

Single-crystal X-ray analysis of a series of 10 silver(I) nitrate complexes containing carbon-rich ligands each composed of a halosubstituted phenyl nucleus bearing a terminal ethynyl group at various positions provided detailed information on the influence of ligand disposition and orientation, coordination preferences, and the co-existence of silver(I)–ethynide and silver(I)–halogen interactions in the construction of coordination networks, which are consolidated by argentophilic and weak intra or intermolecular interactions.

Manuscript received: 22 May 2014.
Manuscript accepted: 23 July 2014.
Published online: 3 September 2014.

Introduction

Coordination polymers are potential precursors for the synthesis of photoluminescent materials,[1] non-linear optical components,[2] and rigid-rod molecular wires.[3] Such polymers are often derived from transitional metal–ethynyl complexes,[4–6] which are regarded as structure building units (SBUs) owing to their occurrence and structural diversity. In the past decades, our group and others have made use of the silver(I)-ethynide[7] supramolecular synthon[8] R–C≡C⊃Ag_n (R = alkyl, phenyl, heteroaryl, n = 3–5) as a versatile and robust SBU in the generation of various high-nuclearity clusters,[9–11] as well as a wide variety of two- and three-dimensional metal–organic frameworks (MOFs).[11,12]

Several years ago, we reported a systematic study on new silver(I) trifluoroacetate complexes containing ligands each composed of a halophenyl nucleus functionalized with a terminal ethynide group, which exhibit a wide variety of crystal structures consolidated by silver–ethynide and silver–halogen interactions.[13] Subsequent investigation of silver(I) complexes generated with aromatic ligands bearing a terminal ethynide substituent showed that crystallization in DMSO in the presence of nitrate ions led to the assembly of argentophilic layer-type structures.[8,14] To extend our systematic investigation in this area, we focussed our attention on the utility of halophenylethynide ligands in combination with nitrate ions for crystallization in DMSO.

Herein, we report the synthesis of a series of 10 new polymeric silver(I) halosubstituted phenyl ethynides, from which 10 crystalline complexes have been generated with the incorporation of nitrate: (*p*-$ClC_6H_4C{\equiv}CAg)_2{\cdot}AgNO_3$ (**1**), (*p*-$BrC_6H_4C{\equiv}CAg)_2{\cdot}AgNO_3$ (**2**), (*p*-$IC_6H_4C{\equiv}CAg)_2{\cdot}AgNO_3$ (**3A** and **3B**), (*m*-$ClC_6H_4C{\equiv}CAg)_2{\cdot}AgNO_3$ (**4**), (*m*-$BrC_6H_4C{\equiv}CAg)_2{\cdot}AgNO_3$ (**5**), (*m*-$IC_6H_4C{\equiv}CAg)_2{\cdot}AgNO_3{\cdot}H_2O$ (**6**), (*o*-$ClC_6H_4C{\equiv}CAg)_2{\cdot}AgNO_3$ (**7**), (*o*-$BrC_6H_4C{\equiv}CAg)_3{\cdot}AgNO_3$ (**8**), and (*o*-$IC_6H_4C{\equiv}CAg)_2{\cdot}AgNO_3{\cdot}$DMSO (**9**). On the basis of our previous experience, dissolution of the crude starting materials [*p*-$ClC_6H_4C{\equiv}CAg]_n$ (**10**), [*p*-$BrC_6H_4C{\equiv}CAg]_n$ (**11**), [*p*-$IC_6H_4C{\equiv}CAg]_n$ (**12**), [*m*-$ClC_6H_4C{\equiv}CAg]_n$ (**13**), [*m*-$BrC_6H_4C{\equiv}CAg]_n$ (**14**), [*m*-$IC_6H_4C{\equiv}CAg]_n$ (**15**), [*o*-$ClC_6H_4C{\equiv}CAg]_n$ (**16**), [*o*-$BrC_6H_4C{\equiv}CAg]_n$ (**17**), and [*o*-$IC_6H_4C{\equiv}CAg]_n$ (**18**) in a concentrated DMSO solution of silver nitrate is expected to generate MOFs stabilized by argentophilic, multinuclear silver(I)–ethynide bonding and silver–halogen interactions, and the phenyl ring is potentially capable of partaking in weak π–π stacking interactions.

Results and Discussion

The polymeric powdery materials [*p*-$ClC_6H_4C{\equiv}CAg]_n$ (**10**), [*p*-$BrC_6H_4C{\equiv}CAg]_n$ (**11**), [*p*-$IC_6H_4C{\equiv}CAg]_n$ (**12**), [*m*-$ClC_6H_4C{\equiv}CAg]_n$ (**13**), [*m*-$BrC_6H_4C{\equiv}CAg]_n$ (**14**), [*m*-$IC_6H_4C{\equiv}CAg]_n$ (**15**), [*o*-$ClC_6H_4C{\equiv}CAg]_n$ (**16**), [*o*-$BrC_6H_4C{\equiv}CAg]_n$ (**17**), and [*o*-$IC_6H_4C{\equiv}CAg]_n$ (**18**) were synthesized from the reaction between the corresponding halosubstituted phenylethynide compounds and silver nitrate in the presence of triethylamine. These precursors were then each dissolved in a concentrated DMSO solution of $AgNO_3$ to increase the silver(I) ion concentration and provide the auxiliary NO_3^- ligand, which are necessary for the formation of the R–C≡C⊃Ag_n supramolecular synthon, where n can be as high as 4 or 5.[15,16]

Description of Crystal Structures

*(p-$ClC_6H_4C{\equiv}CAg)_2{\cdot}AgNO_3$ (**1**)*

Complex **1** contains two crystallographically independent ethynide ligands that exhibit different coordination modes: μ_4–$\eta^1,\eta^1,\eta^2,\eta^2$ for C1≡C2 and μ_3–η^1,η^1,η^2 for C9≡C10 (Fig. 1a). Silver(I) ions Ag2 and Ag3, and their inversion-related equivalents Ag2A and Ag3A constitute a pyramidal Ag_4 segment.

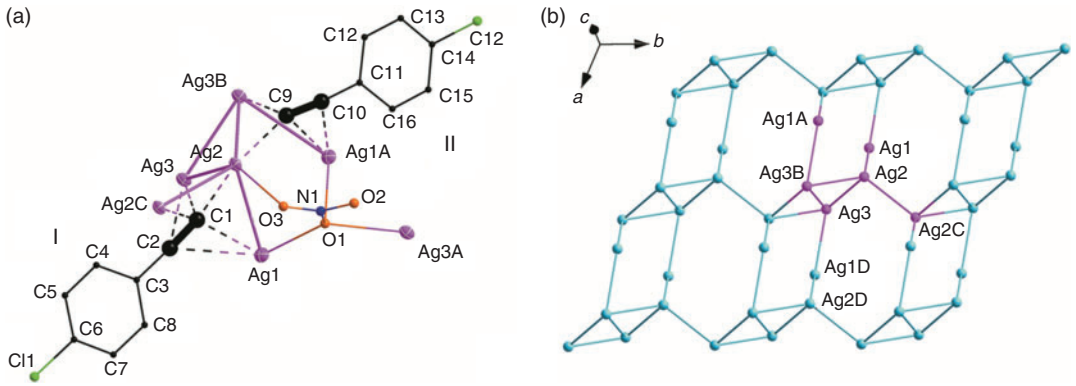

Fig. 1. (a) Perspective view of coordination geometry in double salt (p-$ClC_6H_4C{\equiv}CAg)_2{\cdot}AgNO_3$ (**1**). The argentophilic Ag···Ag distances shown as thick rods lie in the range 2.70–3.40 Å. Silver ions are drawn as thermal ellipsoids (50 % probability level) with atom labelling. (b) Perspective view of silver(I) layer viewed along the c axis. Symmetry codes: A: $-x, -y, 1-z$, B: $1-x, -y, 1-z$, C: $1-x, 1-y, 1-z$, D: $1+x, y, z$. In this and all other figures, silver ions coordinated by independent ethynide ligands are shown in purple, and other symmetry-related silver ions are drawn in blue; the hydrogen and fluorine atoms are omitted for clarity.

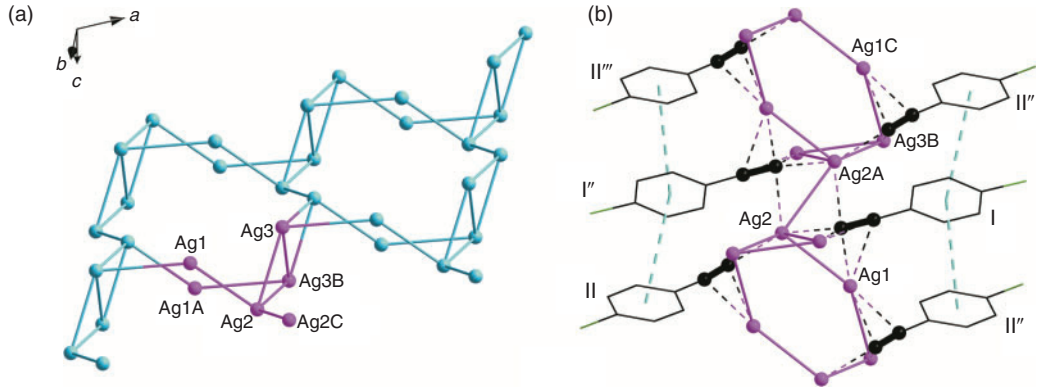

Fig. 2. (a) Perspective view of silver(I) layer in **1** along the b axis. (b) Perspective view of the crystal packing in **1**, showing all notable π–π stacking interactions. Symmetry codes: A: $-x, -y, 1-z$, B: $1+x, y, z$, C: $1-x, 1-y, 1-z$, D: $x, 1+y, z$, E: $1+x, 1+y, z$.

Such segments are linked through argentophilic interaction between type Ag2 ions to generate an infinite silver(I) chain along the b axis. Adjacent chains are further associated by Ag1 ions to yield a wavy layer structure (Fig. 1b and Fig. 2a).

In addition, each argentophilic layer is flanked on both sides by 4-chlorophenyl rings, which exhibit continuous offset face-to-face π–π stacking interactions (inter-centroid distance: ring I···ring II′, 3.915(2) Å; ring I···ring II″, 3.839(2) Å) (Fig. 2b).

(p-$BrC_6H_4C{\equiv}CAg)_2{\cdot}AgNO_3$ (**2**) and (m-$BrC_6H_4C{\equiv}CAg)_2{\cdot}AgNO_3$ (**5**)

Complexes **2** and **5** were found to be isomorphs of the corresponding chlorosubstituted phenylethynide complexes **1** and **4** respectively, and their crystal structures are reported in the Supplementary Material.

(p-$IC_6H_4C{\equiv}CAg)_4{\cdot}(AgNO_3)_2$ (**3A**)

The asymmetric unit of **3A** contains six crystallographically independent Ag^I ions, four ethynide ligands in different ligation modes, and two bridging nitrate ligands in μ_3–η^1,η^3 and μ_3–η^1,η^2 modes. The four independent ethynide groups (C1≡C2, C9≡C10, C17≡C18, C25≡C26) are inserted to separate Ag_3 units in either μ_3–η^1,η^2,η^2 or μ_3–η^1,η^1,η^2 modes (Fig. 3a, b). The independent silver(I) ions coalesce to yield an Ag_6 cluster unit.

Such units are then fused together through argentophilic interaction to yield a silver(I) layer (Fig. 4a). Adjacent phenyl rings of p-$IC_6H_4C{\equiv}C^-$ ligands arranged on both sides of the silver(I) layer are held tightly through both offset face-to-face π–π stacking (inter-centroid distance: ring II···ring III′, 3.884(2) Å; ring IV″···ring I‴, 3.978(2) Å) and edge-to-face C–H···π interactions (C16–H···ring I‴′, 2.735(2) Å with an angle of 134.8°; C20B–H···ring IV″, 2.744(2) Å with an angle of 128.9°) (Fig. 4b).

(p-$IC_6H_4C{\equiv}CAg)_2{\cdot}AgNO_3$ (**3B**)

Unlike **3A**, which was crystallized from slow diffusion by water layering over a DMSO filtrate, complex **3B** was obtained from slow evaporation of a saturated solution of p-$IC_6H_4C{\equiv}CAg$ (**12**) with $AgNO_3$ (3 mmol) in acetonitrile. Complex **3B** belongs to the higher-symmetry space group $P4/mcc$. The independent p-$IC_6H_4C{\equiv}C^-$ ligand is attached to independent silver(I) ions Ag1 and Ag2 in the μ_3–η^1,η^1,η^2 coordination mode (Fig. 5a), in which Ag2 exhibits half-site occupancy. With a two-fold axis passing through the centre of Ag1, an infinite silver(I) chain is generated along the c axis, which is consolidated by the nitrate ligand adopting the μ_2-O,O' mode (Fig. 5b).

Furthermore, adjacent silver(I) chains are interassociated through a notable Ag···I interaction (I1···Ag1B, 3.586(9) Å)[13]

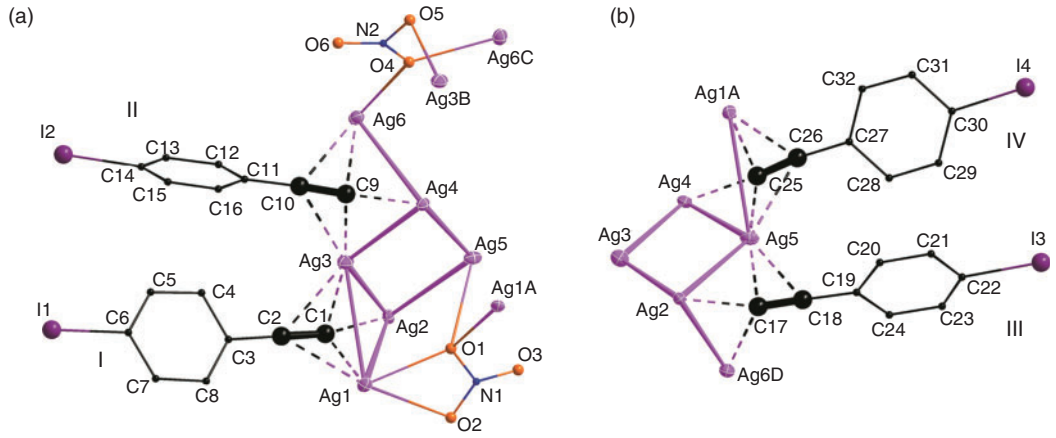

Fig. 3. (a) Perspective view of coordination geometry of two independent ligands in double salt $(p\text{-}IC_6H_4C{\equiv}CAg)_4{\cdot}(AgNO_3)_2$ (**3A**). The argentophilic Ag···Ag distances shown as thick rods lie in the range 2.70–3.40Å. Silver ions are drawn as thermal ellipsoids (50 % probability level) with atom labelling. (b) Perspective view of the remaining ligands in **3A**. Symmetry codes: A: $0.5+x$, $0.5-y$, $1-z$, B: $1+x$, y, z, C: $0.5+x$, $1.5-y$, $1-z$, D: $-0.5+x$, $1.5-y$, $1-z$.

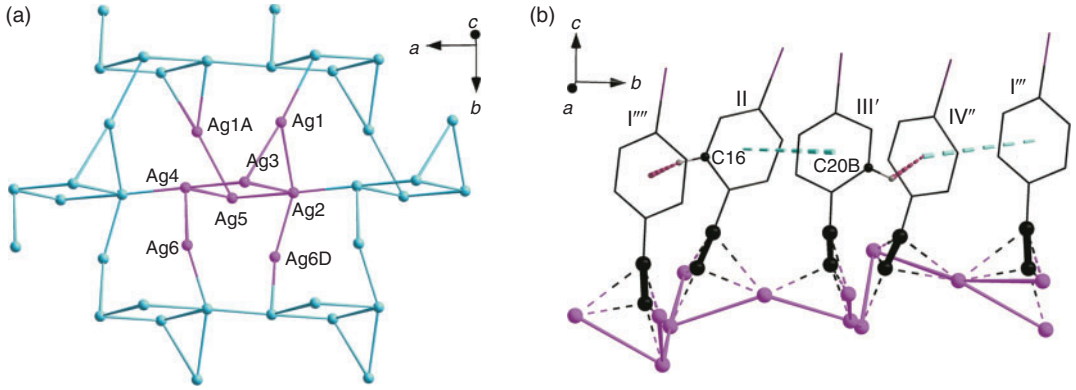

Fig. 4. (a) Perspective view of silver(I) layer in **3A**. (b) Perspective view of the crystal packing in **3A**, showing all notable π–π stacking and C−H···π interactions. Symmetry codes: A: $0.5+x$, $0.5-y$, $1-z$, B: $0.5+x$, $1.5-y$, $1-z$.

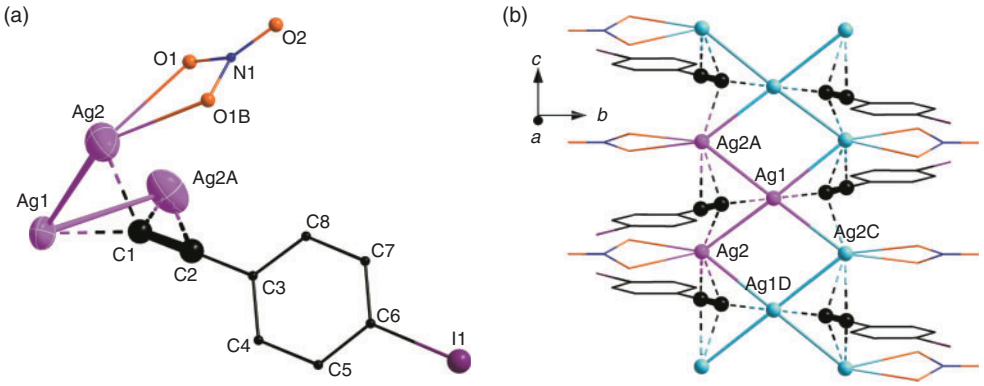

Fig. 5. (a) Perspective view of coordination geometry in double salt $(p\text{-}IC_6H_4C{\equiv}CAg)_2{\cdot}AgNO_3$ (**3B**). The argentophilic Ag···Ag distances shown as thick rods lie in the range 2.70–3.40 Å. Silver ions are drawn as thermal ellipsoids (50 % probability level) with atom labelling. (b) Perspective view of the infinite silver(I) chain in **3B**. Symmetry codes: A: $-x$, y, $0.5+z$, B: $-x$, y, $0.5-z$, C: $-x$, $1-y$, z, D: x, $1-y$, $0.5-z$.

to yield a porous three-dimensional coordination network (Fig. 6a), which is further stabilized by offset face-to-face π–π stacking interaction between phenyl rings (inter-centroid distance: 3.743(7) Å).

After exclusion of the van der Waals radii of the surface atoms, the free area of the nearly circular cross-section of each channel (radius 3.49 Å) in **3B** is ~12.2π Å^2 (Fig. 6b). A calculation with *PLATON* reveals that the free volume of the

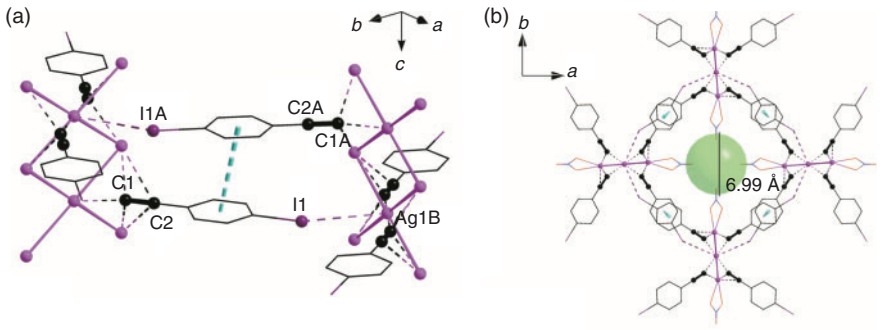

Fig. 6. (a) Perspective view of the interconnection between adjacent silver(I) chains of **3B**, showing all notable Ag···I interactions and π–π stacking interactions. (b) Perspective view of the porous three-dimensional coordination network, showing a cross-section of the empty channel. Symmetry codes: A: x, y, $0.5-z$, B: x, $1-y$, z.

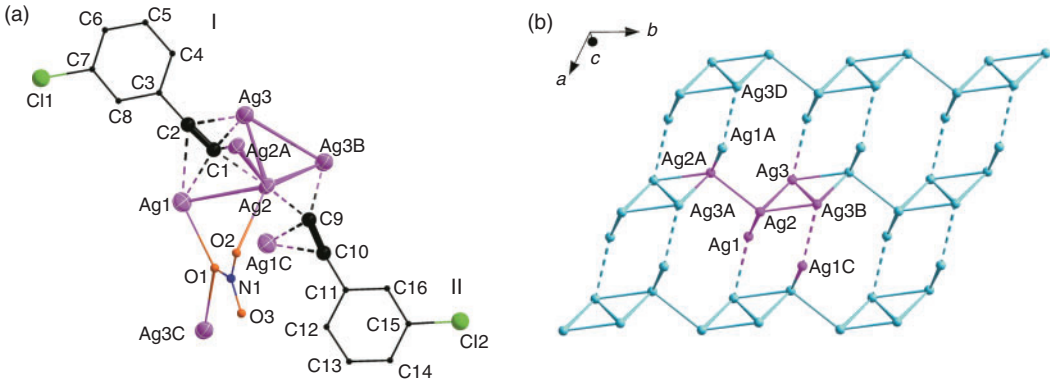

Fig. 7. (a) Perspective view of coordination geometry in double salt (m-$ClC_6H_4C{\equiv}CAg)_2{\cdot}AgNO_3$ (**4**). The argentophilic Ag···Ag distances shown as thick rods lie in the range 2.70–3.40 Å. Silver ions are drawn as thermal ellipsoids (50 % probability level) with atom labelling. (b) Perspective view of the argentophilic silver(I) layer in **4**. Symmetry codes: A: $-x$, $-y$, $1-z$, B: $-x$, $1-y$, $1-z$, C: $1-x$, $1-y$, $1-z$, D: $-1-x$, $-y$, $1-z$.

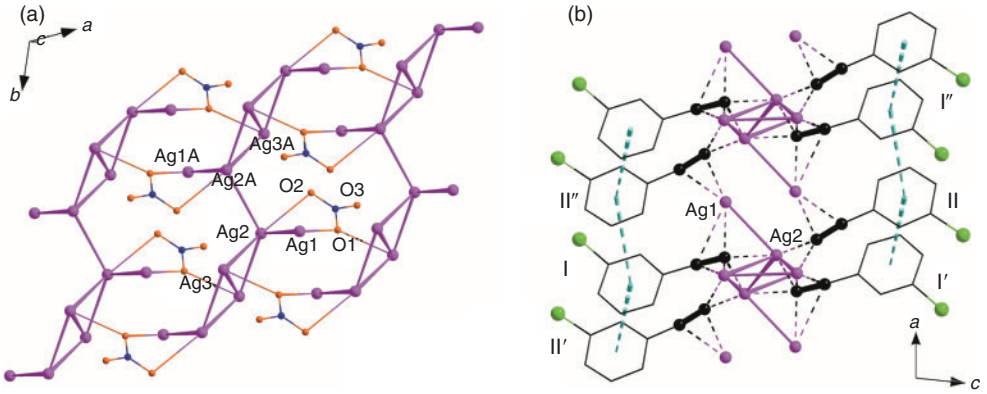

Fig. 8. (a) Perspective view of coordination geometry of the nitrate ligands in **4**. (b) Perspective view of the argentophilic layer in **4** along the b axis, showing all notable π–π stacking interactions. Symmetry code: A: $-x$, $-y$, $1-z$.

channels is 302 $Å^3$ per unit cell. However, no cocrystallized solvent molecule was found within the crystal lattice.

$(m\text{-}ClC_6H_4C{\equiv}CAg)_2{\cdot}AgNO_3$ (**4**)

Complex **4** is isostructural with isomeric complex **1**, both belonging to the same space group $P1$ (no. 2) with very similar unit cell dimensions and matching atomic coordinates. The two independent ethynide moieties exhibit different coordination modes: μ_4–$\eta^1,\eta^1,\eta^2,\eta^2$ for C1≡C2 and μ_3–η^1,η^1,η^2 for C9≡C10 (Fig. 7a). An infinite zigzag silver(I) chain is formed along the b axis through argentophilic interaction between Ag2 and Ag2A. Such chains are interconnected by weak Ag···Ag interaction between Ag1A and Ag3D (3.421(6) Å) along the a axis to generate an argentophilic layer (Fig. 7b).

This layer structure is consolidated by nitrate ligands in μ_3–η^1,η^2 mode (Fig. 8a) and is further stabilized by continuous offset face-to-face π–π stacking interaction between phenyl rings (inter-centroid distance: ring I···ring II′, 3.804(3) Å; ring I···ring II″, 4.107(3) Å) (Fig. 8b).

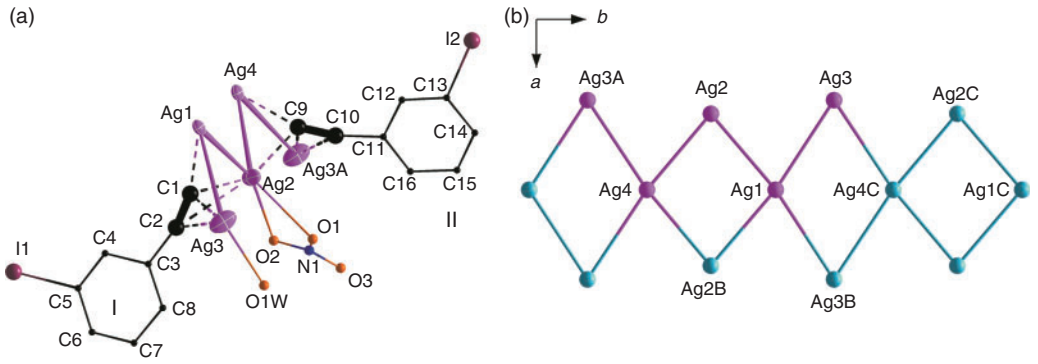

Fig. 9. (a) Perspective view of coordination geometry in double salt (*m*-$IC_6H_4C{\equiv}CAg)_2{\cdot}AgNO_3{\cdot}H_2O$ (**6**). The argentophilic Ag···Ag distances shown as thick rods lie in the range 2.70–3.40 Å. Silver ions are drawn as thermal ellipsoids (30 % probability level) with atom labelling. (b) Perspective view of infinite silver(I) chain in **6**. Symmetry codes: A: $x, -1+y, z$, B: $2-x, y, 1.5-z$, C: $x, 1+y, z$.

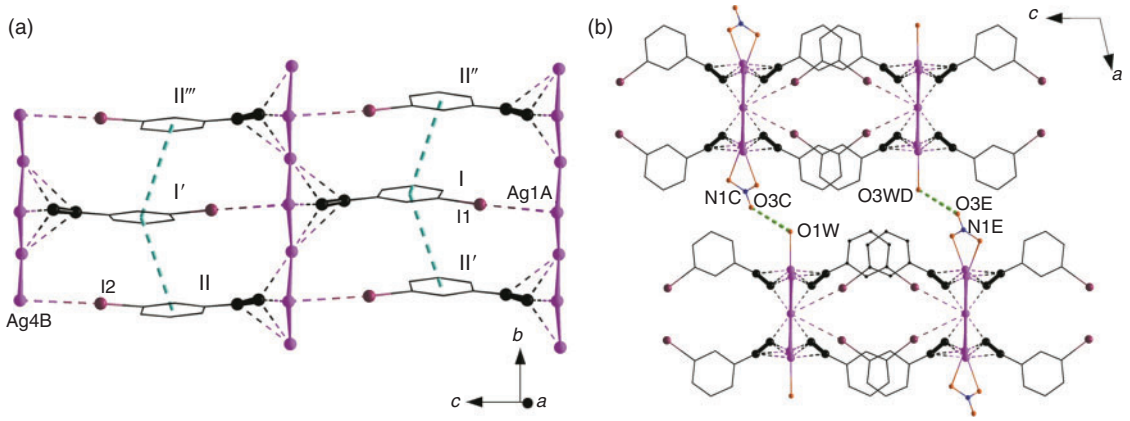

Fig. 10. (a) Perspective view of crystal packing in **6**, showing all notable π–π stacking interactions. (b) Perspective view of the crystal packing showing all notable H-bonding between aqua ligands and nitrate groups between coordination layers. Symmetry codes: A: $2-x, 2-y, 1-z$, B: $2-x, 1-y, 2-z$, C: $1.5-x, 0.5+y, 1.5-z$, D: $1.5-x, 2.5-y, 1-z$, E: $x, 2-y, -0.5+z$.

(m-$IC_6H_4C{\equiv}CAg)_2{\cdot}AgNO_3{\cdot}H_2O$ (**6**)

In the crystal structure of complex **6**, two independent *m*-$IC_6H_4C{\equiv}C^-$ ligands are coordinated to a W-shaped Ag_5 unit, in which C1≡C2 and C9≡C10 adopt μ_3–η^1,η^2,η^2 and μ_3–η^1,η^1,η^2 modes respectively (Fig. 9a). With a two-fold axis passing through type Ag1 and Ag4 ions, the W-shaped Ag_5 units are fused through atom sharing to generate an infinite chain of linked parallelograms along the *b* axis (Fig. 9b).

Adjacent chains are linked by weak Ag···I interactions (I1···Ag1A, 3.49(2) Å and I2···Ag4B, 3.50(1) Å) to generate a layer structure, which is further stabilized by continuous offset face-to-face π–π stacking interaction between phenyl rings (inter-centroid distance: ring I···ring II′, 3.852(8) Å; ring I···ring II″, 3.857(8) Å) (Fig. 10a). Cross-linkage of adjacent metal–organic layers through additional H-bonding between nitrate groups and aqua ligands (O1W···O3C, 2.97(3) Å) yields a 3D supramolecular network (Fig. 10b).

(o-$ClC_6H_4C{\equiv}CAg)_2{\cdot}AgNO_3$ (**7**)

In complex **7**, there are two independent ethynide moieties, each bonded to an Ag_3 triangle via the μ_3–η^1,η^2,η^2 mode, which are fused to an Ag_5 assembly by sharing the Ag3 atom (Fig. 11a). The independent nitrate ion is coordinated to the silver segment in the μ_4–η^1,η^1,η^2 mode. Such Ag_5 segments coalesce to form an infinite silver column along the *a* axis (Fig. 11b).

Adjacent silver(I) columns are assembled in a pseudo-hexagonal array (Fig. 12a) and interconnected through additional H-bonding (C5–H···O3B, 2.69(5) Å) to yield a three-dimensional supramolecular network (Fig. 12b), which is further stabilized by weak Ag···Cl interactions (Ag3D···Cl1C, 3.373(2) Å, Ag2···Cl2, 3.178(2) Å).

(o-$BrC_6H_4C{\equiv}CAg)_3{\cdot}AgNO_3$ (**8**)

In complex **8**, there are three independent ethynide ligands coordinated to an Ag_7 unit (comprising an Ag1–Ag4 segment and symmetry-related silver ions Ag2A, Ag2C, and Ag3B) in different coordination modes: μ_3–η^1,η^1,η^2 for C1≡C2, μ_3–η^1,η^2,η^2 for C9≡C10, and μ_3–η^1,η^1,η^1 for C17≡C18 (Fig. 13a). Two inversion-related Ag_4 segments are fused to yield an Ag_8 rhombic prism. With successive inversion centres located between silver atom pairs (Ag3A and Ag3B), adjacent Ag_8 prisms are interconnected through a double argentophilic link (Ag4···Ag3B, 3.237(7) Å) to produce an infinite silver(I) chain of polyhedra along the *a* axis (Fig. 13b).

Each silver–ethynide coordination chain is further stabilized by continuous offset face-to-face π–π stacking interaction between adjacent phenyl rings of two independent ethynides (inter-centroid distances: ring I···ring II′, 3.895(2) Å; ring II···ring I″, 3.989(2) Å) (Fig. 14a). Subsequently, adjacent

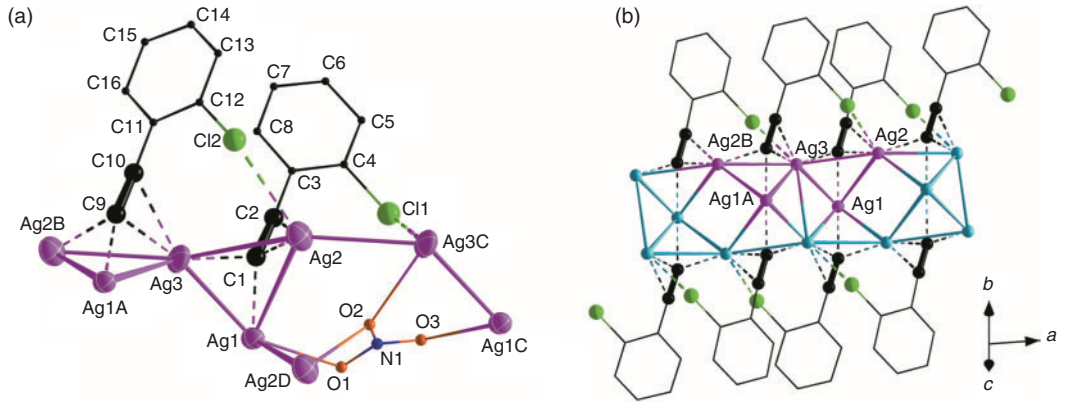

Fig. 11. (a) Perspective view of coordination geometry in double salt (o-$ClC_6H_4C{\equiv}CAg)_2{\cdot}AgNO_3$ (**7**). The argentophilic Ag···Ag distances shown as thick rods lie in the range 2.70–3.40 Å. Silver ions are drawn as thermal ellipsoids (50 % probability level) with atom labelling. (b) Perspective view of infinite silver column coordinated by o-chlorophenylethynide ligands on both sides. Symmetry codes: A: $1-x, -y, 2-z$, B: $-1+x, y, z$, C: $1+x, y, z$, D: $2-x, -y, 2-z$.

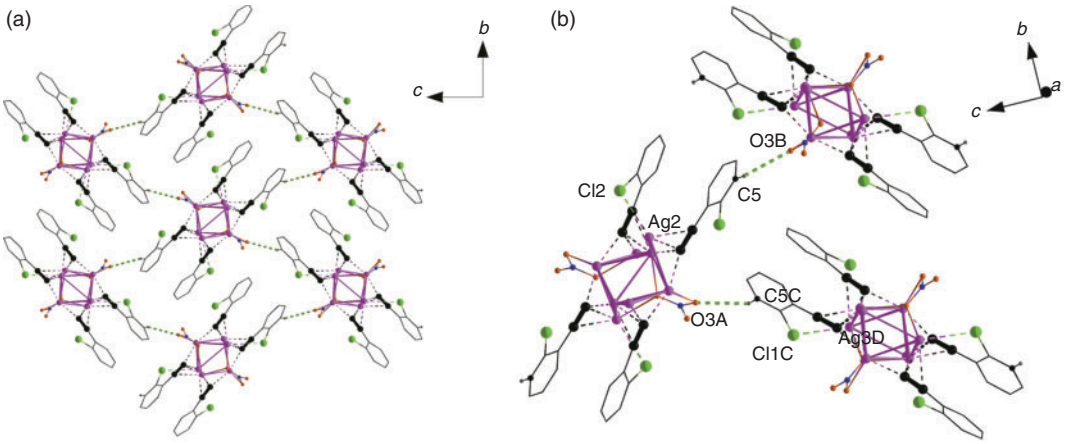

Fig. 12. (a) Perspective view of the pseudo-hexagonal array of the infinite columns in **7** along the a axis, showing all notable H-bonding interactions. (b) Perspective view of interconnection of adjacent chains in **7**. Symmetry codes: A: $-1+x, y, z$, B: $2.5-x, 0.5+y, 1.5-z$, C: $1.5-x, -0.5+y, 1.5-z$, D: $0.5-x, -0.5+y, 1.5-z$.

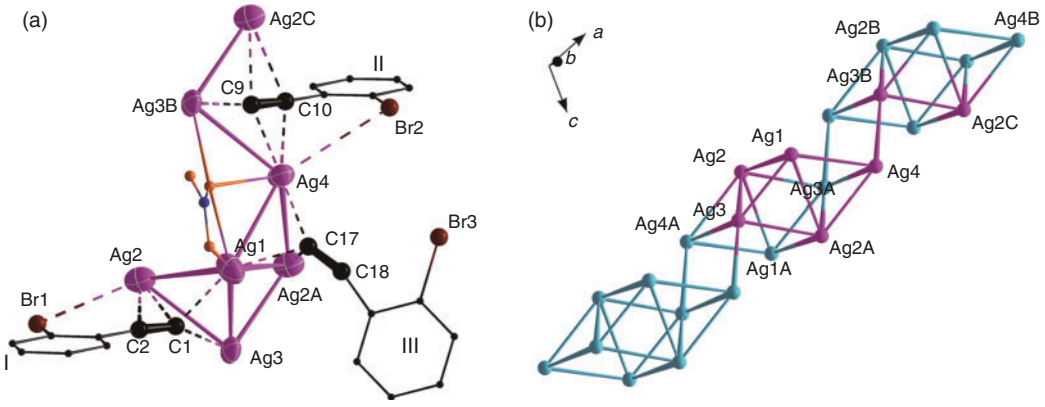

Fig. 13. (a) Perspective view of coordination geometry in double salt (o-$BrC_6H_4C{\equiv}CAg)_3{\cdot}AgNO_3$ (**8**). The argentophilic Ag···Ag distances shown as thick rods lie in the range 2.70–3.40 Å. Silver ions are drawn as thermal ellipsoids (50 % probability level) with atom labelling. (b) Perspective view of the infinite chain of linked polyhedra in **8**. Symmetry codes: A: $-x, 1-y, 1-z$, B: $1+x, y, z$, C: $1-x, 1-y, 1-z$.

polyhedral silver(I) columns are linked by π–π stacking involving the third independent ethynide (inter-centroid distance: ring III′···III″, 3.706(2) Å), hydrogen bonding between the nitrate ions and the phenyl ring of o-$BrC_6H_4C{\equiv}C^-$ ligands (C5B–H···O2A, 2.94(7) Å), which is further stabilized by Ag···Br interaction (Ag2A···Br1A, 3.23(7) Å; Ag4C···Br2C, 3.54(7) Å) to construct a 3D supramolecular network (Fig. 14b).

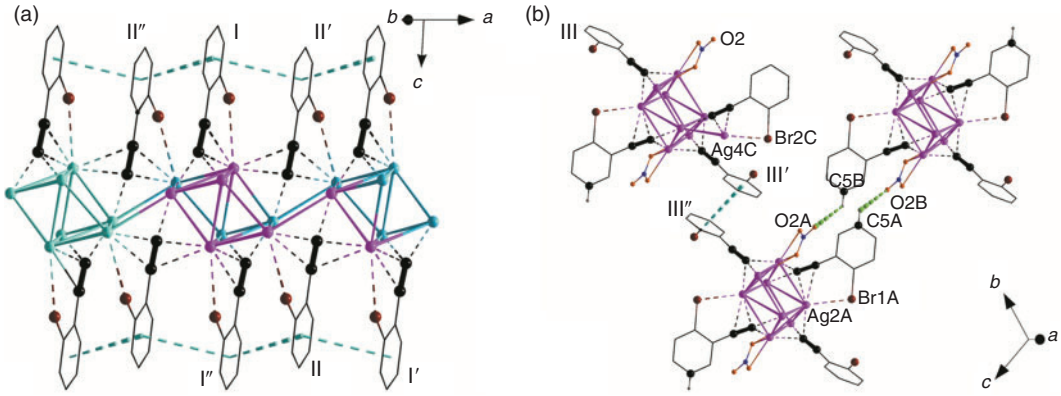

Fig. 14. (a) Perspective view of the crystal packing in **8**, showing continuous π–π stacking interactions. (b) Perspective view of the crystal packing in **8**, showing all notable H-bonding. Symmetry codes: A: $x, -1+y, z$, B: $-x, -y, -z$, C: $1-x, 1-y, 1-z$.

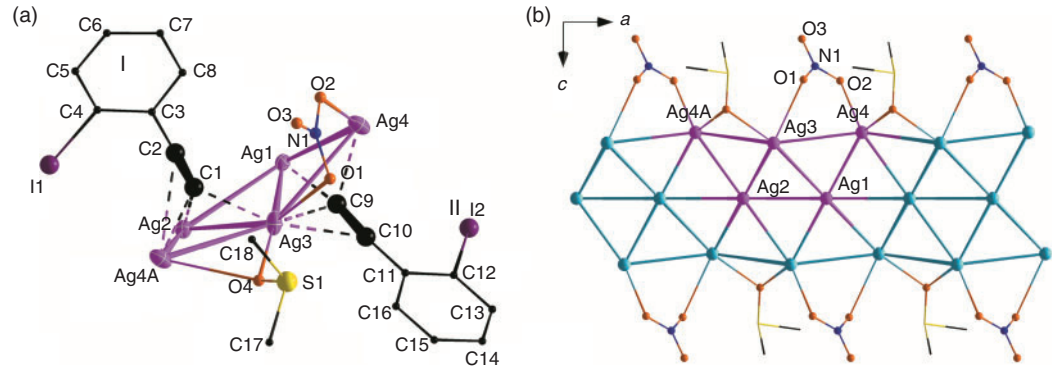

Fig. 15. (a) Perspective view of coordination geometry in double salt (o-$IC_6H_4C{\equiv}CAg)_2{\cdot}AgNO_3{\cdot}$DMSO (**9**). The argentophilic Ag···Ag distances shown as thick rods lie in the range 2.70–3.40 Å. Silver ions are drawn as thermal ellipsoids (50 % probability level) with atom labelling. (b) Perspective view of the wide silver(I) ribbon in **9**. Symmetry code: A: $-1+x, y, z$.

*(o-$IC_6H_4C{\equiv}CAg)_2{\cdot}AgNO_3{\cdot}$DMSO (**9**)*

As illustrated in Fig. 15a, both ethynide moieties of the two independent ligands are each attached to an Ag_3 basket in μ_3–η^1,η^1,η^2 coordination mode. These two Ag_3 segments coalesce to produce an Ag_5 aggregate through sharing one silver atom, Ag3. With successive centres lying on silver ions Ag1 and Ag2, such Ag_5 aggregates are fused to form a wide silver(I) ribbon consisting of three strands along the *a* axis (Fig. 15b), which is further consolidated by μ_2-coordinated nitrate and μ_2-coordinated DMSO ligands.

In addition, adjacent silver(I) ribbons are linked through weak H-bonding between nitrate and DMSO ligands (C17A–H···O1B, 2.68(2) Å) to form a supramolecular layer structure (Fig. 16). Such layers are interconnected by offset face-to-face π–π stacking interactions between phenyl rings (inter-centroid distance: ring I′···II″, 3.793(2) Å). As a result, a complex, three-dimensional silver(I) organic supramolecular network structure is constructed.

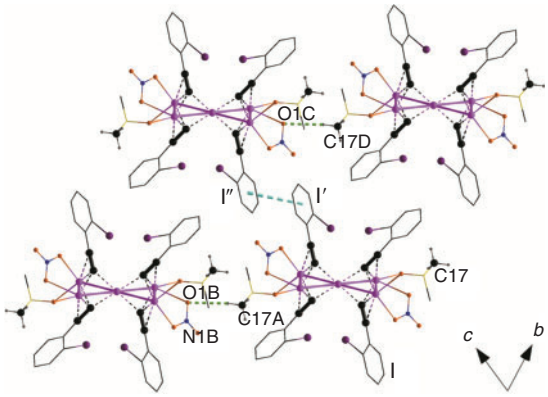

Fig. 16. Perspective view of crystal packing in **9**, showing all notable H-bonding and π–π stacking interactions. Symmetry codes: A: $1-x, -y, 1-z$, B: $x, -1+y, 1+z$, C: $x, y, 1+z$, D: $1-x, 1-y, 1-z$.

Structure Correlation Relationship

The series of 10 complexes reported herein reaffirms the general utility of the silver–ethynide supramolecular synthon $R{-}C{\equiv}C{\supset}Ag_n$ ($n=4$, 5) in coordination network assembly. Except for **3B**, which exists as a three-dimensional porous coordination network, all complexes were crystallized from slow liquid diffusion of deionized water into the respective DMSO filtrate. Silver(I)-layer formation is facilitated by multinuclear Ag–C and argentophilic interactions in **1**, **2**, **3A**, **4**, and **5** (Fig. 17). With the terminal ethynide and halosubstituent having a *para* relationship, the size difference between bromo and chloro groups is not sufficient to influence layer-structure construction in **1** and **2**. On switching to the sterically bulky iodo substituent in complex **3A**, a more closely packed three-dimensional coordination network is obtained.

Similarly, the layer structures of **4** and **5** based on *meta*-$XC_6H_4C{\equiv}C^-$ ligands (X = Cl, Br respectively) do not differ much on comparison. In addition, formation of an infinite coordination chain becomes more favourable as the

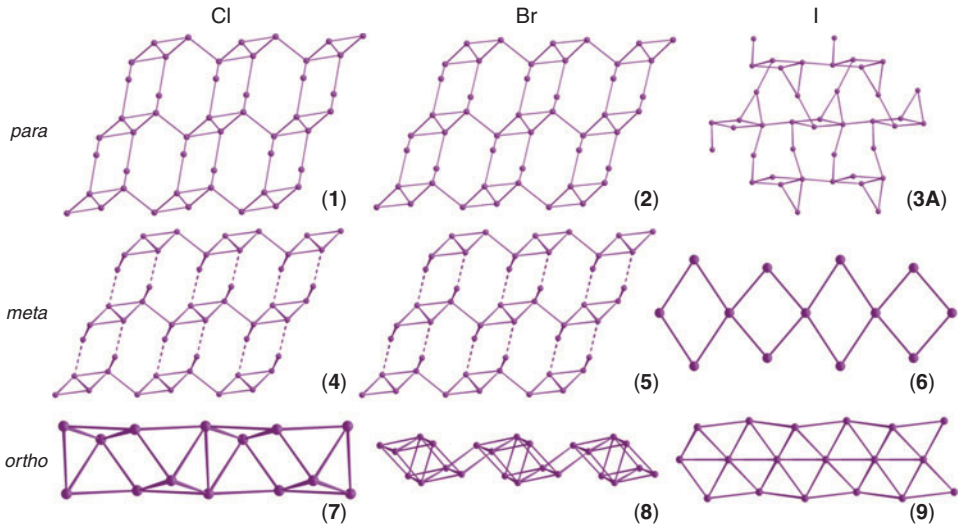

Fig. 17. Argentophilic silver(I) structures in complexes **1**–**9**, except **3B**.

halosubstituent of the phenylethynide is changed to the iodo group in **6**. However, when the terminal ethynide and halosubstituent are positioned close to each other, silver–chloro and silver–bromo interactions occur in **7** and **8** respectively, whereas no silver–iodo interaction is found in **9** owing to steric hindrance. Consequently, silver(I) columnar structures are found in **7** and **8** in contrast to the ribbon in **9**.

Weak Intermolecular Interactions and Formation of Supramolecular Frameworks

Among the 10 complexes reported herein, DMSO is only found as a cocrystallized solvent molecule in complex **9**. This result reflects the dominant coordination capacity of the nitrate ion, which plays a major role in directing two-dimensional argentophilic assembly. The coordination modes of the nitrate groups vary from the common μ_3–η^1,η^2 kind to the μ_2–η^1,η^1 and μ_4–η^1,η^1,η^2 varieties. The nitrate ligand generally plays two important roles: one type spans an edge of the Ag_n basket to consolidate the $[Ag_nC{\equiv}C]^{(n-1)+}$ cationic moiety, whereas the other type bridges adjacent Ag_n baskets or Ag ions to generate an infinite chain or a layer-type structure.

In complexes **1**–**5**, the offset face-to-face π–π stacking interactions and edge-to-face C–H···π interactions play significant roles in stabilizing the argentophilic silver(I) layers. In **6**, **8**, and **9**, aromatic π–π stacking interaction between adjacent layers leads to the generation of a three-dimensional supramolecular network. When the terminal ethynide (C1≡C2) is positioned closer to the chloro group (**7**), the stronger Ag···Cl interaction dominates formation of the assembled structure at the expense of weak π–π stacking interactions.

Hydrogen bonding between the nitrate group and the aqua ligand in **6**, or weak C–H···O interaction (**7**–**9**) with the phenyl ring confer enhanced stability to the silver(I) coordination chains and connect them into a two- or three-dimensional supramolecular network.

Conclusion

The present work reports the structural characterization of a series of 10 silver(I) nitrate complexes containing carbon-rich ligands each composed of a halosubstituted phenyl nucleus bearing a terminal ethynyl group at various positions. Single-crystal X-ray analysis of the complexes provided detailed information on the influence of ligand disposition and orientation, coordination preferences, and co-existence of different kinds of silver(I)–ethynide and silver(I)–halogen interactions in coordination network construction, as well as the roles played by weak interactions in supramolecular assembly.

Experimental

Materials and General Methods

(4-Iodophenylethynyl)trimethylsilane, (3-iodophenylethynyl) trimethylsilane, (2-iodophenylethynyl)trimethylsilane, (4-bromophenylethynyl)trimethylsilane, (3-bromophenylethynyl) trimethylsilane, (2-bromophenylethynyl)trimethylsilane, 4-chlorophenyl acetylene, 3-chlorophenyl acetylene, and 2-chlorophenyl acetylene were obtained commercially from Farco Chemical Supplies or Aldrich and used without further purification. Organic solvents were removed under reduced pressure on a rotary evaporator. Chromatographic purification of the products was performed on Macherey Nagel Kieselgel 60M (230–400 mesh). Thin-layer chromatography (TLC) was conducted on Merck silica gel 60 F_{254} (0.1-mm thickness) coated on aluminium plates. Melting points (uncorrected) were measured with a Reichert apparatus in degrees Celsius. Elemental analysis (C, H, N) was performed at Shanghai Institute of Organic Chemistry, China.

CAUTION! Silver ethynide complexes are potentially explosive and should be handled with extreme care and used in small quantities.

Preparation of Polymeric Silver Salts as Synthetic Precursors

*$[p\text{-}ClC_6H_4C{\equiv}CAg]_n$ (**10**), $[p\text{-}BrC_6H_4C{\equiv}CAg]_n$ (**11**), $[p\text{-}IC_6H_4C{\equiv}CAg]_n$ (**12**), $[m\text{-}ClC_6H_4C{\equiv}CAg]_n$ (**13**), $[m\text{-}BrC_6H_4C{\equiv}CAg]_n$ (**14**), $[m\text{-}IC_6H_4C{\equiv}CAg]_n$ (**15**), $[o\text{-}ClC_6H_4C{\equiv}CAg]_n$ (**16**), $[o\text{-}BrC_6H_4C{\equiv}CAg]_n$ (**17**), and $[o\text{-}IC_6H_4C{\equiv}CAg]_n$ (**18**)*

In a 10-mL round bottom flask, silver nitrate (1 mmol) was added to a solution of acetonitrile or methanol (40 mL) that contained an equimolar amount of halosubstituted phenyl acetylene and triethylamine (1 mmol). After vigorous stirring for 2 h, the yellow precipitate was collected by filtration and washed

thoroughly with 3 × 20 mL methanol. ν_{max} (KBr)/cm^{-1} ($\nu_{C\equiv C}$, w) 2050, **10**; 2048, **11**; 2034, **12**; 2010, **13**; 2010, **14**; 2031, **15**; 2025, **16**; 2024, **17**; 2018, **18**.

*General Procedure for Crystallization of Silver Ethynide Complexes **1**, **2**, **3A**, and **4**–**9** via Slow Liquid Diffusion*

$AgNO_3$ (0.510 g, 3 mmol) was first dissolved in DMSO (1 mL), and polymeric $[AgC\equiv CR]_n$ (~100 mg) was then added to the solution. After stirring until all solids had dissolved, the solution was filtered and the filtrate transferred to a test-tube. De-ionized water was layered over the filtrate, which was stored in the dark. Crystals of good quality were deposited after 1 week by slow liquid diffusion of water into the filtrate.

*(p-$ClC_6H_4C\equiv CAg)_2{\cdot}AgNO_3$ (**1**)*

Colourless plate-like crystals in ~75 % yield. Anal. calc. for $C_{16}H_8Ag_3Cl_2NO_3$: C 29.26, H 1.23, N 2.13; found C 29.67, H 1.47, N 1.91. ν_{max} (KBr)/cm^{-1} 2007 (w, $\nu_{C\equiv C}$). Compound **1** decomposes above 220°C.

*(p-$BrC_6H_4C\equiv CAg)_2{\cdot}AgNO_3$ (**2**)*

Colourless plate-like crystals of in ~75 % yield. Anal. calc. for $C_{16}H_8Ag_3Br_2NO_3$: C 25.77, H 1.08, N 1.88; found C 25.41, H 1.29, N 1.58. ν_{max} (KBr)/cm^{-1} 2000 (w, $\nu_{C\equiv C}$). Compound **2** decomposes above 220°C.

*(p-$IC_6H_4C\equiv CAg)_4{\cdot}(AgNO_3)_2$ (**3A**)*

Yellow plate-like crystals of **3A** were deposited in ~60 % yield. Anal. calc. for $C_{32}H_{16}Ag_6I_4N_2O_6$: C 22.89, H 0.96, N 1.67; found C 22.81, H 1.07, N 1.41. ν_{max} (KBr)/cm^{-1} 2019 (w, $\nu_{C\equiv C}$). Compound **3A** decomposes above 200°C.

*(p-$IC_6H_4C\equiv CAg)_2{\cdot}AgNO_3$ (**3B**)*

$AgNO_3$ (0.510 g, 3 mmol) was dissolved in 1 mL acetonitrile. Then $[p\text{-}IC_6H_4C\equiv CAg]_n$ (~55 mg) was added to the solution. After stirring for approximately half an hour, the solution was filtered and the filtrate stored at −10°C in a refrigerator. One day later, yellow needle-like crystals of **3B** were deposited in ~45 % yield. Anal. calc. for $C_{16}H_8Ag_3I_2NO_3$: C 22.89, H 0.96, N 1.67; found C 22.80, H 1.02, N 1.48. ν_{max} (KBr)/cm^{-1} 2013 (w, $\nu_{C\equiv C}$). Compound **3B** decomposes above 200°C.

*(m-$ClC_6H_4C\equiv CAg)_2{\cdot}AgNO_3$ (**4**)*

Colourless plate-like crystals in ~75 % yield. Anal. calc. for $C_{16}H_8Ag_3Cl_2NO_3$: C 29.26, H 1.23, N 2.13; found C 28.77, H 1.34, N 2.21. ν_{max} (KBr)/cm^{-1} 2006 (w, $\nu_{C\equiv C}$). Compound **4** decomposes above 200°C.

*(m-$BrC_6H_4C\equiv CAg)_2{\cdot}AgNO_3$ (**5**)*

Pale yellow plate-like crystals in ~75 % yield. Anal. calc. for $C_{16}H_8Ag_3Br_2NO_3$: C 25.77, H 1.08, N 1.88; found C 25.61, H 1.18, N 1.68. ν_{max} (KBr)/cm^{-1} 2037 (w, $\nu_{C\equiv C}$). Compound **5** decomposes above 200°C.

*(m-$IC_6H_4C\equiv CAg)_2{\cdot}AgNO_3{\cdot}H_2O$ (**6**)*

Colourless needle-like crystals in ~5 % yield. Compound **6** decomposes above 200°C.

*(o-$ClC_6H_4C\equiv CAg)_2{\cdot}AgNO_3$ (**7**)*

Colourless needle-like crystals of **7** in ~65 % yield. Anal. calc. for $C_{16}H_8Ag_3Cl_2NO_3$: C 29.26, H 1.23, N 2.13; found

Table 1. Crystallographic data and structure refinement parameters of complexes 1–9
Space group $P2_1/n$ is equivalent to standard $P2_1/c$ by an axial transformation

Complex	**1**	**2**	**3A**	**3B**	**4**	**5**	**6**	**7**	**8**	**9**
Structural formula	$C_{16}H_8Ag_3Cl_2NO_3$	$C_{16}H_8Ag_3Br_2NO_3$	$C_{32}H_{16}Ag_6I_4N_2O_6$	$C_{16}H_8Ag_3I_2NO_3$	$C_{16}H_8Ag_3Cl_2NO_3$	$C_{16}H_8Ag_3Br_2NO_3$	$C_{16}H_{10}Ag_3I_2NO_4$	$C_{16}H_8Ag_3Cl_2NO_3$	$C_{24}H_{12}Ag_4Br_3NO_3$	$C_{18}H_{14}Ag_3I_2NO_4S$
Formula weight	656.74	745.66	1679.29	839.64	656.74	745.66	857.66	656.74	2067.11	917.77
Crystal system	Triclinic	Triclinic	Orthorhombic	Tetragonal	Triclinic	Triclinic	Monoclinic	Monoclinic	Triclinic	Triclinic
Space group	*P*1 (no. 2)	*P*1 (no. 2)	$P2_12_12_1$ (no. 19)	*P*4/*mcc* (no. 124)	*P*1 (no. 2)	*P*1 (no. 2)	*C*2/*c* (no. 15)	$P2_1/n$ (no. 14)	*P*1 (no. 2)	*P*1 (no. 2)
a [Å]	6.767(5)	6.823(7)	7.578(5)	17.995(3)	6.919(7)	6.954(3)	25.612(6)	6.407(2)	7.093(5)	6.414(4)
b [Å]	6.910(5)	7.040(8)	11.504(8)	17.995(3)	7.014(8)	7.053(4)	7.309(2)	11.654(3)	13.352(1)	13.747(1)
c [Å]	19.148(2)	19.588(2)	42.093(3)	7.340(2)	18.449(2)	18.710(1)	21.164(5)	23.463(7)	14.913(1)	14.235(1)
α [Å]	97.609(2)	96.787(3)	90.0	90.0	94.193(2)	93.845(1)	90.0	90.0	111.505(2)	63.875(1)
β [Å]	92.859(2)	95.259(3)	90.0	90.0	93.830(2)	93.607(1)	102.979(5)	97.233(4)	99.310(1)	86.037(1)
γ [Å]	111.981(1)	112.744(2)	90.0	90.0	112.370(10)	112.416(1)	90.0	90.0	99.169(2)	80.216(1)
V [Å^3]	818.1(1)	852.3(2)	3669.5(4)	2376.9(7)	821.5(2)	842.5(8)	3860.4(2)	1738.0(8)	1259.3(2)	1110.45(1)
Z	2	2	4	4	2	2	8	4	1	2
ρ_c [gcm^{-3}]	2.666	2.905	3.040	2.346	2.655	2.939	2.951	2.510	2.726	2.745
μ [mm^{-1}]	3.897	8.116	6.550	5.056	3.881	8.210	6.233	3.669	7.852	5.518
R_1^A ($I > 2\sigma$)	0.0332	0.0242	0.0485	0.0349	0.0221	0.0193	0.1061	0.0325	0.0304	0.0146
wR_2^B (all data)	0.0980	0.0731	0.1309	0.1273	0.0737	0.0694	0.3020	0.0556	0.0669	0.0346
GOF	1.187	1.205	1.173	1.217	1.143	1.182	1.098	1.026	1.032	1.114

[A] $R_1 = \Sigma||F_o| - |F_c||/\Sigma|F_o|$.
[B] $wR_2 = \{\Sigma[w(F_o^2 - F_c^2)^2]/\Sigma[w(F_o^2)^2]\}^{1/2}$.

C 29.42, H 1.06, N 2.36. ν_{max} (KBr)/cm^{-1} 2022 (w, $\nu_{C\equiv C}$). Compound **7** decomposes above 180°C.

*(o-BrC$_6$H$_4$C≡CAg)$_3$·AgNO$_3$ (**8**)*

Colourless needle-like crystals of **8** in ~50 % yield. Anal. calc. for $C_{24}H_{12}Ag_4Br_3NO_3$: C 27.89, H 1.17, N 1.36; found C 27.68, H 1.21, N 1.42. ν_{max} (KBr)/cm^{-1} 2016 (w, $\nu_{C\equiv C}$). Compound **8** decomposes above 180°C.

*(o-IC$_6$H$_4$C≡CAg)$_2$·AgNO$_3$·DMSO (**9**)*

Yellow needle crystals of **9** in ~50 % yield. Anal. calc. for $C_{18}H_{14}Ag_3I_2NO_4S$: C 23.56, H 1.54, N 1.53; found C 23.67, H 1.47, N 1.61. ν_{max} (KBr)/cm^{-1} 2011 (w, $\nu_{C\equiv C}$). Compound **9** melts from 162.4 to 164.1°C.

X-Ray Crystallographic Study

Selected crystals were used for intensity data collection on a Bruker AXS Kappa Apex II Duo diffractometer at 296 K using frames of oscillation range 0.3°, with $2° < \theta < 28°$. As crystals of complex **6** are rather brittle and easily shattered by cutting, a fairly large one was selected for data collection, which accounts for the abnormally low precision of the structure analysis. A multiscan absorption correction was applied to all measured intensity data using the *SADABS* program.[17] The structures were solved by the direct method and refined by full-matrix least-squares on F^2 using the *SHELXTL* program package.[18] The crystallographic data are summarized in Table 1. CCDC 1015550–1015559 contain the crystallographic data for this paper, which can be obtained free of charge from the Cambridge Crystallographic Data Centre via www.ccdc.cam.ac.uk/data_request/cif.

Supplementary Material

Descriptions of crystal structures **2** and **5** are available on the Journal's website.

Acknowledgements

We gratefully acknowledge financial support by the Hong Kong Research Grants Council (GRF CUHK 402710), the Wei Lun Foundation, and the award of a Postgraduate Studentship to P.-C. Cheng and a Postdoctoral Research Fellowship to S. C. K. Hau respectively from The Chinese University of Hong Kong.

References

[1] (a) S. Barlow, D. O'Hare, *Chem. Rev.* **1997**, *97*, 637. doi:10.1021/CR960083V
(b) I. R. Whittall, A. M. McDonagh, M. G. Humphrey, *Adv. Organomet. Chem.* **1998**, *42*, 291. doi:10.1016/S0065-3055(08)60545-6
(c) M. P. Cifuentes, M. G. Humphrey, *J. Organomet. Chem.* **2004**, *689*, 3968. doi:10.1016/J.JORGANCHEM.2004.06.027

[2] (a) M. Younus, A. Kohler, S. Cron, N. Chawdhury, M. R. A. Al-Madani, M. S. Khan, N. J. Long, R. H. Friend, P. R. Raithby, *Angew. Chem. Int. Ed.* **1998**, *37*, 3036. doi:10.1002/(SICI)1521-3773(19981116)37:21<3036::AID-ANIE3036>3.0.CO;2-R
(b) V. W.-W. Yam, *Acc. Chem. Res.* **2002**, *35*, 555. doi:10.1021/AR0000758
(c) Q.-H. Wei, L.-Y. Zhang, G.-Q. Yin, L.-X. Shi, Z.-N. Chen, *J. Am. Chem. Soc.* **2004**, *126*, 9940. doi:10.1021/JA047302B
(d) H.-B. Xu, L.-X. Shi, E. Ma, L.-Y. Zhang, Q.-H. Wei, Z.-N. Chen, *Chem. Commun.* **2006**, 1601. doi:10.1039/B602222G
(e) H.-B. Xu, J. Ni, K.-J. Chen, L.-Y. Zhang, Z.-N. Chen, *Organometallics* **2008**, *27*, 5665. doi:10.1021/OM8005883
(f) H.-B. Xu, L.-Y. Zhang, J. Ni, H.-Y. Chao, Z.-N. Chen, *Inorg. Chem.* **2008**, *47*, 10744. doi:10.1021/IC800733X
(g) H.-B. Xu, L.-Y. Zhang, X.-M. Chen, X.-L. Li, Z.-N. Chen, *Cryst. Growth Des.* **2009**, *9*, 569. doi:10.1021/CG800866R

[3] (a) F. Paul, C. Lapinte, *Coord. Chem. Rev.* **1998**, *178–180*, 431. doi:10.1016/S0010-8545(98)00150-7
(b) V. W.-W. Yam, K. M.-C. Wong, *Top. Curr. Chem.* **2005**, *257*, 1. doi:10.1007/B136069
(c) S. Rigaut, C. Olivier, K. Costuas, S. Choua, O. Fadhel, J. Massue, P. Turek, J. Y. Saillard, P. H. Dixneuf, D. Touchard, *J. Am. Chem. Soc.* **2006**, *128*, 5859. doi:10.1021/JA0603453
(d) G. A. Koutsantonis, G. I. Jenkins, P. A. Schauer, B. Szczepaniak, B. W. Skelton, C. Tan, A. H. White, *Organometallics* **2009**, *28*, 2195. doi:10.1021/OM800992P
(e) K. J. Kilpin, M. L. Gower, S. G. Telfer, G. B. Jameson, J. D. Crowley, *Inorg. Chem.* **2011**, *50*, 1123. doi:10.1021/IC1020059

[4] (a) P. Braunstein, C. Frison, N. Oberbeckmann-Winter, X. Morise, A. Messaoudi, M. Bénard, M.-M. Rohmer, R. Welter, *Angew. Chem. Int. Ed.* **2004**, *43*, 6120. doi:10.1002/ANIE.200461291
(b) T. K. Ronson, T. Lazarides, H. Adams, S. J. A. Pope, D. Sykes, S. Faulkner, S. J. Coles, M. B. Hursthouse, W. Clegg, R. W. Harrington, M. D. Ward, *Chem. – Eur. J.* **2006**, *12*, 9299. doi:10.1002/CHEM.200600698
(c) D. Salazar-Mendoza, S. A. Baudron, M. W. Hosseini, *Chem. Commun.* **2007**, 2252. doi:10.1039/B704466F
(d) C. Fernández-Cortabitarte, F. García, J. V. Morey, M. McPartlin, S. Singh, A. E. H. Wheatley, D. S. Wright, *Angew. Chem. Int. Ed.* **2007**, *46*, 5425. doi:10.1002/ANIE.200700925

[5] (a) M. I. Bruce, *Chem. Rev.* **1991**, *91*, 197. doi:10.1021/CR00002A005
(b) H. Lang, D. S. A. George, G. Rheinwald, *Coord. Chem. Rev.* **2000**, *206–207*, 101. doi:10.1016/S0010-8545(00)00270-8
(c) N. J. Long, C. K. Williams, *Angew. Chem. Int. Ed.* **2003**, *42*, 2586. doi:10.1002/ANIE.200200537
(d) V. W.-W. Yam, *J. Organomet. Chem.* **2004**, *689*, 1393. doi:10.1016/J.JORGANCHEM.2003.12.029
(e) S. S. Y. Chui, M. F. Y. Ng, C.-M. Che, *Chem. – Eur. J.* **2005**, *11*, 1739. doi:10.1002/CHEM.200400881
(f) W.-Y. Wong, *Coord. Chem. Rev.* **2007**, *251*, 2400. doi:10.1016/J.CCR.2007.01.006

[6] (a) C. P. McArdle, J. J. Vittal, R. J. Puddephatt, *Angew. Chem. Int. Ed.* **2000**, *39*, 3819. doi:10.1002/1521-3773(20001103)39:21<3819::AID-ANIE3819>3.0.CO;2-6
(b) C. P. McArdle, M. C. Jennings, J. J. Vittal, R. J. Puddephatt, *Chem. – Eur. J.* **2001**, *7*, 3572. doi:10.1002/1521-3765(20010817)7:16<3572::AID-CHEM3572>3.0.CO;2-C
(c) C. P. McArdle, M. J. Irwin, M. C. Jennings, J. J. Vittal, R. J. Puddephatt, *Chem. – Eur. J.* **2002**, *8*, 723. doi:10.1002/1521-3765(20020201)8:3<723::AID-CHEM723>3.0.CO;2-T
(d) C. P. McArdle, S. Van, M. C. Jennings, R. J. Puddephatt, *J. Am. Chem. Soc.* **2002**, *124*, 3959. doi:10.1021/JA012006+
(e) F. Mohr, M. C. Jennings, R. J. Puddephatt, *Eur. J. Inorg.* **2003**, 217.
(f) T. J. Burchell, M. C. Jennings, R. J. Puddephatt, *Inorg. Chim. Acta* **2006**, *359*, 2812. doi:10.1016/J.ICA.2005.10.030
(g) N. C. Habermehl, D. J. Eisler, C. K. Kirby, N. L.-S. Yue, R. J. Puddephatt, *Organometallics* **2006**, *25*, 2921. doi:10.1021/OM0601706

[7] The term 'silver–ethynide' is preferred to 'silver–ethynyl' because the silver–carbon bonding interaction is considered to be mainly ionic with minor covalent σ and π components; the negative charge residing mainly on the terminal C atom draws neighboring Ag^I ions close to one another to facilitate the onset of argentophilic Ag···Ag interactions. See: T. C. W. Mak, L. Zhao, X.-L. Zhao, in *The Importance of Pi-Interactions in Crystal Engineering* (Eds E. R. T. Tiekink, J. Zukerman-Schpector) **2012**, Ch. 13, pp. 323–366 (Wiley: Chichester, UK), and references cited therein.

[8] (a) G. R. Desiraju, *Angew. Chem. Int. Ed. Engl.* **1995**, *34*, 2311. doi:10.1002/ANIE.199523111
(b) A. Nangia, G. R. Desiraju, *Top. Curr. Chem.* **1998**, *198*, 57. doi:10.1007/3-540-69178-2_2
(c) G. R. Desiraju, *Angew. Chem. Int. Ed.* **2007**, *46*, 8342. doi:10.1002/ANIE.200700534

(d) P.-S. Cheng, S. Marivel, S.-Q. Zang, G.-G. Gao, T. C. W. Mak, *Cryst. Growth Des.* **2012**, *12*, 4519. doi:10.1021/CG300691N
(e) T. Hu, T. C. W. Mak, *Inorg. Chem.* **2013**, *52*, 9066. doi:10.1021/IC401259R

[9] (a) P. Pyykkö, *Chem. Rev.* **1988**, *88*, 563. doi:10.1021/CR00085A006
(b) P. Pyykkö, *Chem. Rev.* **1997**, *97*, 597. doi:10.1021/CR940396V
(c) P. Pyykkö, *Chem. Soc. Rev.* **2008**, *37*, 1967. doi:10.1039/B708613J
(d) S. Grimme, J.-P. Djukic, *Inorg. Chem.* **2010**, *49*, 2911. doi:10.1021/IC9024662
(e) J. Muñiz, C. Wang, P. Pyykkö, *Chem. – Eur. J.* **2011**, *17*, 368. doi:10.1002/CHEM.201001765

[10] V. W. W. Yam, W. K. M. Fung, K. K. Cheung, *Angew. Chem. Int. Ed. Engl.* **1996**, *35*, 1100. doi:10.1002/ANIE.199611001

[11] (a) T. C. W. Mak, L. Zhao, *Chem. Asian J.* **2007**, *2*, 456. doi:10.1002/ASIA.200600386
(b) S. C. K. Hau, P.-S. Cheng, T. C. W. Mak, *J. Am. Chem. Soc.* **2012**, *134*, 2922. doi:10.1021/JA211438Q
(c) Y.-P. Xie, T. C. W. Mak, *J. Am. Chem. Soc.* **2011**, *133*, 3760. doi:10.1021/JA1112035
(d) Y.-P. Xie, T. C. W. Mak, *Angew. Chem. Int. Ed.* **2012**, *51*, 8783. doi:10.1002/ANIE.201202195
(e) Z.-G. Jiang, K. Shi, Y.-M. Lin, Q.-M. Wang, *Chem. Commun.* **2014**, 2353. doi:10.1039/C3CC49290G
(f) S. C. K. Hau, T. C. W. Mak, *J. Am. Chem. Soc.* **2014**, *136*, 902. doi:10.1021/JA412095Y

[12] (a) T. Zhang, J. Kong, Y. Hu, X. Meng, H. Yin, D. Hu, C. Ji, *Inorg. Chem.* **2008**, *47*, 3144. doi:10.1021/IC702230H
(b) T. Zhang, H. Song, X. Dai, X. Meng, *Dalton Trans.* **2009**, 7688. doi:10.1039/B905449A
(c) T. Zhang, Y. Hu, J. Kong, X. Meng, X. Dai, H. Song, *CrystEngComm* **2010**, *12*, 3027. doi:10.1039/C002038A
(d) Y. Zhao, P. Zhang, B. Li, X. Meng, T. Zhang, *Inorg. Chem.* **2011**, *50*, 9097. doi:10.1021/IC2012809
(e) Z. Zhang, B. Li, X. Meng, X. Yin, T. Zhang, *Dalton Trans.* **2013**, 4306. doi:10.1039/C2DT32030D

[13] S. M. J. Wang, T. C. W. Mak, *Polyhedron* **2009**, *28*, 2684. doi:10.1016/J.POLY.2009.05.004

[14] P.-S. Cheng, S. C. K. Hau, T. C. W. Mak, *Inorg. Chim. Acta* **2013**, *403*, 110. doi:10.1016/J.ICA.2013.03.014

[15] G.-C. Guo, T. C. W. Mak, *Chem. Commun.* **1999**, 813. doi:10.1039/A901876J

[16] (a) G.-C. Guo, G.-D. Zhou, Q.-G. Wang, T. C. W. Mak, *Angew. Chem. Int. Ed.* **1998**, *37*, 630. doi:10.1002/(SICI)1521-3773(19980316)37:5<630::AID-ANIE630>3.0.CO;2-K
(b) G.-C. Guo, G.-D. Zhou, T. C. W. Mak, *J. Am. Chem. Soc.* **1999**, *121*, 3136. doi:10.1021/JA984117N
(c) Q.-G. Wang, T. C. W. Mak, *J. Am. Chem. Soc.* **2001**, *123*, 1501. doi:10.1021/JA0028727
(d) Q.-M. Wang, T. C. W. Mak, *Angew. Chem. Int. Ed.* **2001**, *40*, 1130. doi:10.1002/1521-3773(20010316)40:6<1130::AID-ANIE11300>3.0.CO;2-T
(e) Q.-M. Wang, T. C. W. Mak, *Chem. Commun.* **2001**, 807. doi:10.1039/B009765I
(f) S. C. K. Hau, T. C. W. Mak, *Chem. – Eur. J.* **2013**, *19*, 5387. doi:10.1002/CHEM.201204225

[17] G. M. Sheldrick, *SADABS: Program for Empirical Absorption Correction of Area Detector Data* **1996** (University of Göttingen: Göttingen, Germany).

[18] G. M. Sheldrick, *SHELXTL 5.10 for Windows: Structure Determination Software Programs* **1997** (Bruker Analytical X-Ray Systems, Inc.: Madison, WI).